High-Quality Compact Interdigital Microstrip Resonator and Its Application to Bandpass Filter

**Boris Belyaev[1, 2], Alexey Serzhantov[2], Aleksandr Leksikov[1, 2],
Yaroslav Bal'va[1], and Andrey Leksikov[1, *]**

Abstract—A compact microstrip resonator based on the interdigital structure is proposed. The resonator has several times higher unloaded quality factor compared to similar resonators presented previously and can even reach the Q-factor of a regular $\lambda/4$ resonator. The size of the resonator can be significantly reduced with a substantial increase in quality factor by incrementing the number of fingers in the interdigital structure. In addition, for each gap between the fingers, there exist an optimal number of fingers that correspond to the maximum Q-factor. An extension of the upper stopband for a bandpass filter designed using the resonator can be achieved by the interconnection of the fingers in each of the comb structures. The simulation results are proven by fabricated resonators and a fourpole bandpass filter. For the central frequency of 2000 MHz and 16.2% fractional bandwidth, the lateral size of the filter is only 11.5 mm × 3.8 mm for alumina substrate (eps = 9.8). The filter has an upper stopband up to $5.8f_0$ at the level −40 dB.

1. INTRODUCTION

Because bandpass filters still occupy a significant place in modern radio systems, it is impossible to carry out a comprehensive downsizing of all types of microwave systems without miniaturizing their main component. Therefore, noticeable effort is still dedicated to the ways of filter miniaturization, and several main approaches can be identified. In planar structures, great attention is attracted to stepped-impedance resonators (SIRs) [1–5] and spiral resonators [6, 7]; also, during the last years, more attention has been directed to complex hairpin, net-type, and interdigital structures [8–15]. These resonators demand accurate technology of fabrication, but the advantages in size and electrical characteristics allow one to create bandpass filters with unique characteristics.

In [9, 10], two ideas of compact hybrid resonators are presented, which allow not only a decrease in the resonator size but also an increase in the width of the upper stopband. In [10], a $\lambda/4$ interdigital structure is presented, whose length is at least half of the length of $\lambda/4$ SIR. At the same time, the proposed resonator has an unloaded quality factor higher than typical interdigital structures.

An idea of tolerant $\lambda/4$ SIR presented in [15] demonstrates an ability to fabricate a four-pole microstrip filter with $5f_0$ width of the stopband at the level of −60 dB. In addition, folding the resonator reduces its size, allowing to achieve a rather compact size of the planar bandpass filter with a central frequency of ~ 1 GHz.

The usage of multimode resonators [16–18] for the fabrication of compact filters is usually limited in the case of multipole filters, as it is hard to obtain a proper matching of a device with feed lines.

The most compact resonators could be created using multilayered structures [19–21]. The appearance of LTCC and analogous technologies allows one to create structures with 10 or even more

[1] Kirensky Institute of Physics, Siberian Branch, Russian Academy of Sciences, Krasnoyarsk 660036, Russia. [2] Siberian Federal University, Krasnoyarsk 660074, Russia.

layers and to reduce the size of a resonator several times. The best results are achieved when ideas developed for planar structures [9] are applied to the multilayered structure [22]. In this case, filters become compact, and the Q-factor of their resonators becomes higher than analogs [23]. However, multilayered structures, especially LTCC-based ones, have strong limitations in postfabrication tuning and possess usually higher in-band loss.

Previously, we have presented an idea of multiconductor resonator and its realizations in multilayer [24] and interdigital microstrip configurations [25, 26]. For the 3-layered structure, a filter is compact and has a wide stopband $(10.5f_0)$ at the $-100\,\text{dB}$ level. For a microstrip interdigital structure [26], it has at least four times higher unloaded Q-factor than other types of compact microstrip resonators.

In this paper, we develop an idea of microstrip interdigital multiconductor resonator. Particularly, in Section 2, we present a theory of multiconductor resonators and its application to the microstrip one. In Section 3, we show how the structural parameters of the resonator influence its characteristics and that an optimal number of fingers exists for each gap between the fingers when a maximum value of unloaded Q-factor is observed. In Section 4, an investigation of the frequency response for a bandpass filter versus a type of tapping is presented, and by finger interconnection, one can make the stopband wider. The results of the fabricated bandpass filters are summarized in Section 5.

2. MULTICONDUCTOR RESONATOR THEORY

The topology of the resonator is presented in Fig. 1(a). It consists of two comb microstrip structures directed opposite to each other, forming thereby the so-called interdigital structure. The common conductor of each comb structure is connected to the ground over its entire length. Each of the fingers in the structure can be considered itself as a quarter-wave resonator. When width of the fingers w and the gaps between them s_g are small compared to the substrate thickness, the electromagnetic coupling between them is strong.

Any microwave resonator at its first oscillation mode can be accurately described as oscillation circuit with inductance L, capacitance C, and resistance R. Its resonant frequency and unloaded Q-factor can be calculated as

$$\omega_0 = \frac{1}{\sqrt{LC}}; \quad Q_0 = \frac{1}{R}\sqrt{\frac{L}{C}}. \tag{1}$$

For two coupled resonators with mutual inductance L_{12} and capacitance C_{12}, whose equivalent circuit is presented in Fig. 1(b), the lower and upper resonant frequencies can be calculated as

$$\omega_e = \frac{1}{\sqrt{(L + L_{12})(C + 2C_{12})}}, \quad \omega_o = \frac{1}{\sqrt{(L - L_{12})C}}. \tag{2}$$

At frequency ω_e, the currents in the inductors flow in the same direction, but the potentials on the capacitor plates of C_{12} have opposite signs. At the same time, at the upper frequency ω_o, the situation is reversed.

The calculations performed for the cases with number of fingers 3, 4, and higher give an analytical equation for the unloaded Q-factor of the lowest resonance and its frequency [26]:

$$Q_N = \sqrt{\frac{N}{2}}Q_2, \quad f_N = \frac{1}{\sqrt{N/2}}f_2\,(N \geq 2), \tag{3}$$

where Q_2 and f_2 are the unloaded quality factor and the resonant frequency of the interdigital structure having two fingers, respectively, and f_N is the frequency of the lowest mode of the resonator with N fingers in the structure.

One can see from Equation (3) that the growth in the number N results in the unloaded Q-factor increases with simultaneous decrease in its resonant frequency. It should be recalled that the equations presented above are suitable only in the case when the width of the fingers and the gaps between them are much smaller than the substrate thickness.

The conclusion drawn based on the interdigital structure's equivalent circuit was proven by electromagnetic simulation in the AWR Design Environment and Sonnet Studio Suite. A dielectric
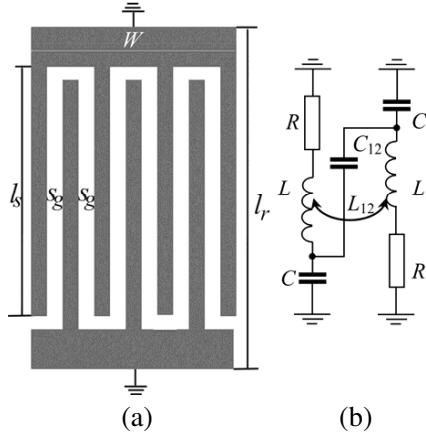
Figure 1. Topology of (a) the resonator and (b) equivalent circuit for the case when the structure has only two fingers.
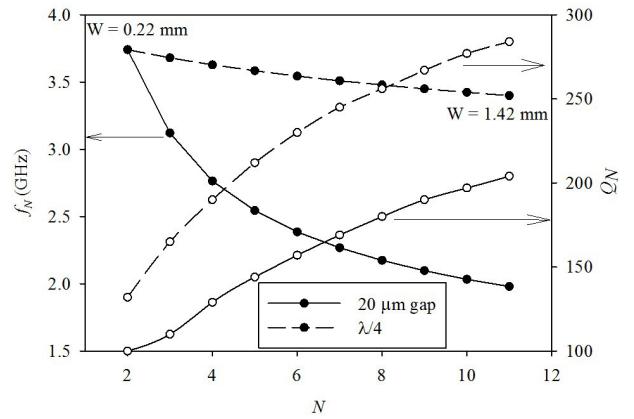
Figure 2. Dependences of the resonant frequency and the unloaded Q-factor versus number of fingers N in the structure.

substrate with $\varepsilon = 9.8$, $\tan\delta = 0.0002$, and thickness $h = 1\,\text{mm}$ was chosen as a base for the copper resonator ($\sigma = 5.88 \times 10^7\,\text{Sm/m}$) having length and width of the fingers of $4.4\,\text{mm}$ and $100\,\mu\text{m}$, respectively, and gaps of $20\,\mu\text{m}$ between them. These correspond to $L = 8.12 \times 10^{-10}\,\text{H/mm}$, $L_{12} = 5.6 \times 10^{-10}\,\text{H/mm}$, $C = 3.02 \times 10^{-13}\,\text{F/mm}$, and $C_{12} = 7.06 \times 10^{-13}\,\text{F/mm}$. The box was chosen without a top cover. The results of the simulation, particularly the dependences of both the unloaded Q-factor and the resonant frequency on N are presented in Fig. 2 by solid line. It can be seen that frequency f_N is significantly reduced, and quality factor Q_N increases with the number of fingers N in the interdigital structure.

The result can be explained as follows: the high-frequency currents in the fingers of interdigital structure flow at the first resonant frequency in the same direction; this is why the summary inductance of all conductors has nearly the same magnitude as the inductance of a single conductor. At the same time, the current distributes uniformly onto all fingers, thereby reducing the resistive loss in the resonator.

For comparison, the dependence of resonant frequency and unloaded Q-factor versus the width of the regular $\lambda/4$ resonator is presented in the same figure by dashed line. The minimal width of the $\lambda/4$ resonator that corresponds to $N = 2$ is $0.42\,\text{mm}$, and the maximum width (11 fingers) is $1.42\,\text{mm}$.

3. RESONATOR CHARACTERISTICS

In Equation (3), the unlimited rise of N leads to an analogous growth in the unloaded Q-factor. Indeed, as shown below, an optimal number of fingers N depending on the overall resonator's width and gap S_g exists.

It is well known that the microstrip resonator unloaded Q-factor decreases with the decrease in the resonator width due to increased current density in the resonator resulting in increased ohmic losses. Radiation loss increases in this case, too, amplifying the effect. However, an unexpected behavior of the Q-factor is observed in this case. In Fig. 3, a dependence of the Q-factor on the number of fingers N obtained by the simulation is shown. The simulation was carried out with the help of AWR Microwave Office for the width of the resonator fixed at $2\,\text{mm}$. It is obvious that the increase of N when the width of the resonator and gaps s_g are constant is possible only at the expense of decreasing the total cross-section of fingers. In other words, the Q-factor in this case should decrease. However, in Fig. 3(a) there is 34% growth of the Q-factor with an increase of the number of fingers from 2 to 23. At the same time, a further increase of the number N leads to a decrease in the Q, and already at 75 fingers ($7\,\mu\text{m}$ width of a finger), the Q-factor is 89 (30% less for 2 fingers). Therefore, an optimal number of fingers exists, which corresponds to a maximum value of the unloaded Q-factor.
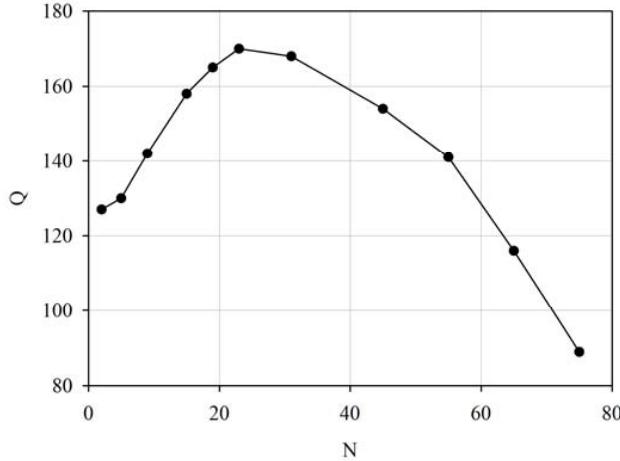
Figure 3. Dependence of the unloaded Q-factor versus number of fingers N in the structure for a fixed width of the resonator.
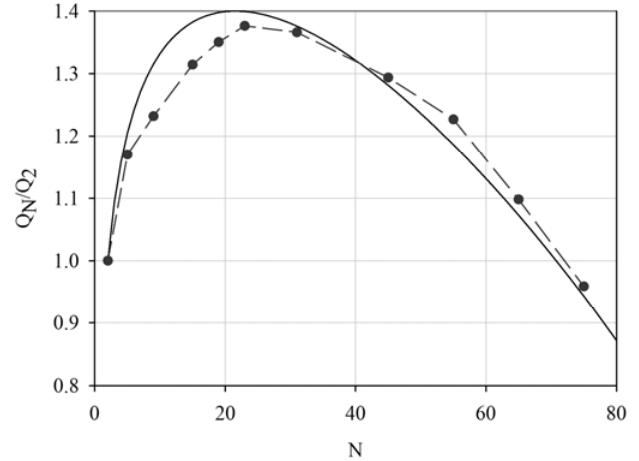
Figure 4. Comparison of Q-factor dependences obtained by analytical equations (solid line) and electromagnetic simulation (dash line).

Therefore, an analytical calculation of the unloaded Q-factor versus resonator parameters was made to explain the existence of its optimal value. An equivalent circuit similar to the one used above (Fig. 1) was employed with the same approximation of strong inductive coupling between the fingers.

The unloaded Q-factor of a resonator can be calculated as

$$Q_N = \frac{Z_{eqvN}}{R_N} = \frac{1}{R_N}\sqrt{\frac{L_N}{C_N}}, \tag{4}$$

where R_N is an equivalent resistance of the resonator that can be calculated as

$$R_N = kR_s\frac{l_s}{W_{eff}}, \tag{5}$$

k is an unknown coefficient that depends on the current profile in the finger, R_S the surface resistance, l_s the finger's length, and W_{eff} the effective width of resonator calculated as

$$W_{eff} = Nw = W - (N-1)s_g. \tag{6}$$

From Kirchhoff equations, one can find that, for N-coupled inductors, the total inductance is:

$$L_N = \frac{L + (N-1)L_{ij}}{N} \tag{7}$$

At the same time, for the case of strong inductive coupling $L_{ij} \approx L$, it means that the total (equivalent) inductance appears to be $L_N \approx L$.

An inductance per unit length of a microstrip line with low dielectric permittivity of substrate can be approximately found as [27]

$$L \approx \mu_0 \ln\left(\frac{8h}{w}\right), \tag{8}$$

where h is the thickness of the line substrate and w the width of the microstrip line. Then, L_N may be determined as follows:

$$L_N \approx \mu_0 \ln\left(\frac{8h}{w}\right) = \mu_0 \ln\left(\frac{8Nh}{W-(N-1)s_g}\right). \tag{9}$$

For a transmission line filled with air ($\varepsilon = 1$), per unit length inductance and capacitance can be calculated as

$$C = \frac{1}{c^2}\frac{1}{L}. \tag{10}$$

It means that the equivalent capacitance of the multiconductor resonator is

$$C_N = NC = \frac{N}{c^2 L} = \frac{N}{\mu_0 c^2 \ln \left(\dfrac{8Nh}{W - (N-1)s_g} \right)}. \tag{11}$$

The more the number of fingers N is, the more the value of the equivalent resonator's capacitance is. Therefore, on increasing N, one has to maintain the resonant frequency as constant for the comparison of the Q-factor values to be correct. In the first instance, the resonant frequency is determined by finger's length, whose dependence on N may be written as

$$l_s(N) \approx l_r \frac{1}{c\sqrt{L_N C_N}} = l_r \frac{1}{c\sqrt{L_N \dfrac{N}{c^2 L_N}}} = l_r \frac{1}{\sqrt{N}}, \tag{12}$$

l_r is the finger's length.

Then, the equivalent resistance of the structure is

$$R_N = kR_s \frac{l_s}{W_{eff}} = kR_s \frac{l_r}{\sqrt{N}(W - (N-1)s_g)} \tag{13}$$

Finally, the unloaded quality factor for the resonator with N fingers can be calculated as follows:

$$Q_N = \frac{1}{R_N} \sqrt{\frac{L_N}{C_N}} = \frac{\sqrt{N}[W - (N-1)s_g]}{kR_s l_r} \sqrt{\frac{\dfrac{\mu_0 \ln \left(\dfrac{8Nh}{W - (N-1)s_g} \right)}{N}}{\mu_0 c^2 \ln \left(\dfrac{8Nh}{W - (N-1)s_g} \right)}}$$

$$= \frac{[W - (N-1)s_g]}{kR_s l_r} \mu_0 c \ln \left(\frac{8Nh}{W - (N-1)s_g} \right) \tag{14}$$

$$Q_N = \frac{1}{k} \frac{Z}{R_N} \frac{[W - (N-1)s_g]}{l_r} \ln \left(\frac{8Nh}{W - (N-1)s_g} \right), \tag{15}$$

where $Z = \mu_0 c = \sqrt{\mu_0 / \varepsilon_0}$ is the vacuum wave impedance.

Let us compare the Q-factor of a two-finger structure and a structure with N fingers.

$$\frac{Q_N}{Q_2} = \left[\frac{W - (N-1)s_g}{W - s_g} \right] \frac{\ln \left(\dfrac{8Nh}{W - (N-1)s_g} \right)}{\ln \left(\dfrac{16h}{W - s_g} \right)}. \tag{16}$$

Two trends in Eq. (16) can be observed: the first is a linear decrease of the Q-factor associated with a decrease in the conducting cross-section, which in turn leads to an increase in ohmic losses in the resonator, and the second is a nonlinear (logarithmic) growth of the Q-factor associated with a change of equivalent inductance of the structure. For a small number of fingers, a change in their number causes a higher change of the inductance than the change of the resistance, so a growth of the Q-factor is observed. When the two trends become equivalent, an optimum number of fingers is achieved.

To verify this conclusion, we have carried out a simulation and analytical calculation for a 2 mm width resonator on substrate with $\varepsilon = 2$ and thickness of 1 mm. The chosen gap was 20 μm. During simulation, the resonant frequency was tuned to 1 GHz for each number of fingers. The comparison is presented in Fig. 4. The results obtained by both methods have a similar behavior: more than 34% increase in the Q-factor was observed when N changed from 2 to 22. Further increasing N is accompanied by lowering the Q-factor. Thus, in this case, 22 is the optimal number of fingers. A small difference between the dependencies in the region of small N comes from the fact that a current distribution in the fingers is nonuniform, which was not taken into account in the analytical calculations.

It is obvious that when the resonator's width is constant, the optimum number of fingers will depend on the gap value between them. A computer simulation was performed for 1-mm-wide resonator created
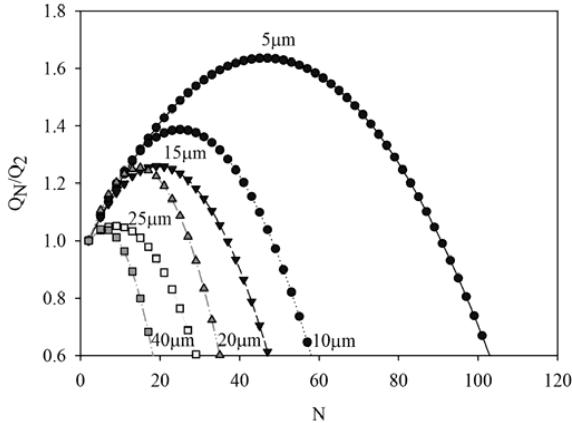
Figure 5. Q-factor versus number of fingers in the structure obtained by analytical equations for different gaps between the fingers.
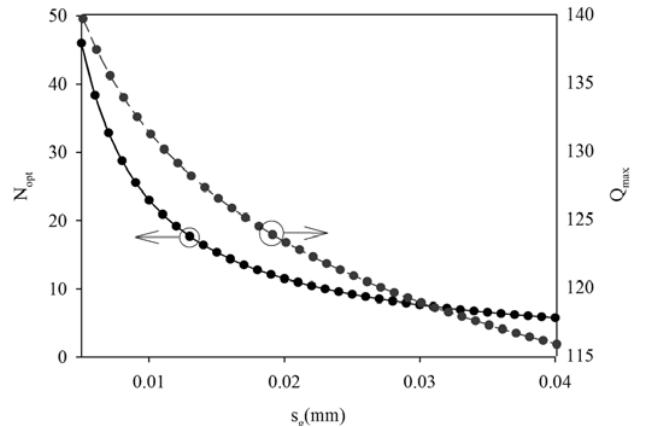
Figure 6. Dependences of the optimal number of fingers and the maximum Q-factor versus a gap between the fingers in the resonator.

on a 1-mm-thick alumina substrate with different gaps between the fingers. The results for $s_g = (40; 25; 20; 15; 10; 5)\,\mu m$ are presented in Fig. 5, and it shows that the decrease of the gap brings a significant increase in both an optimal number of fingers and a maximum value of Q. In Fig. 6, the dependences of the optimal number of fingers and the maximum value of the Q-factor on the gap between the fingers are presented. One can see that an optimal number of fingers has an inverse proportionality to the gap value. At the same time, a 20% growth of the maximum unloaded Q-factor was found for such change in the gap.

The results obtained here and in [26] were used in investigating the behavior of the maximum unloaded Q-factor on the width of the resonator. It is a common knowledge that the unloaded Q-factor of a regular microstrip resonator increases with increasing width. The dependences of the Q-factor versus resonator's width obtained by simulation are shown in Fig. 7 for the three cases. The first one concerns an ordinary microstrip $\lambda/4$ resonator, and the other two are the results with regard to the proposed resonator. Note that in the two last cases, which differ by a value of the gaps (1 and $5\,\mu m$), the Q-factors correspond to the optimal number of fingers N. In Fig. 7, the behavior of the resonator under investigation appears similar to the microstrip $\lambda/4$ one. Besides, the less the gaps are, the closer the Q-factor is to the Q-factor of the ordinary resonator.

In this investigation, a 1-mm-thick alumina substrate was used for the resonators with width from 0.2 to 4 mm. At each width, the resonators were tuned to 1 GHz resonant frequency by changing the resonators' length.

Also an ability to apply the proposed analytical model to obtain the shift of resonant frequency on number of fingers was analyzed. According to the model:

$$\frac{f_1(N)}{f_1(2)} = \sqrt{\frac{2}{N}}, \tag{17}$$

and the shift does not depend on dielectric constant of the substrate. A simulation was performed for the resonator with $s_g = 0.01$ mm designed on a 1 mm substrate with different $\varepsilon = (1, 9.8, 40, 80)$. The results of the simulation are presented in Fig. 8. One can see that the relation $\frac{f_1(N)}{f_1(2)}$ from Equation (17) of the resonant frequency is ε independent. At the same time, the comparison of the result of the simulation with the equation, presented in Fig. 9 shows that for 30 fingers there already exists 10% difference in the shift obtained by analytical model and simulation (in analytical model the shift is bigger). The effect comes from the fact that for such a number of fingers, the fingers situated on the opposite sides of the resonator are already not in the strong inductive coupling ($L_{ij} \neq L$), which mainly has influence on the resonance position, but not on unloaded Q-factor.

Two main conclusions can be drawn. First, the Q-factor of the proposed resonator having an optimal number of fingers is practically the same as in the case of a regular microstrip $\lambda/4$ resonator.
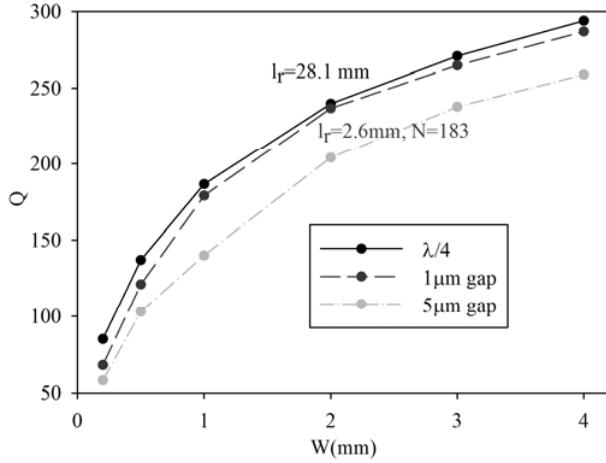
Figure 7. Dependences of the unloaded Q-factor versus width of the resonator. Regular $\lambda/4$ resonator (solid line), proposed resonator with the gap 1 μm (dashed line), and proposed resonator with the gap 5 μm (dashed-dot line).
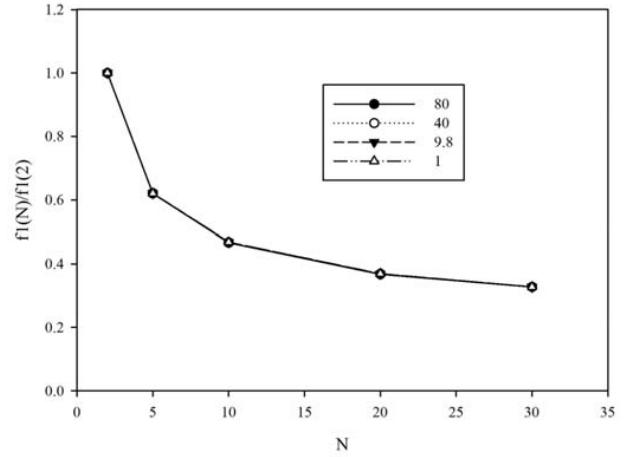

Figure 8. Frequency shift of position of the first oscillation mode on changing N for different dielectric constant of the substrate.
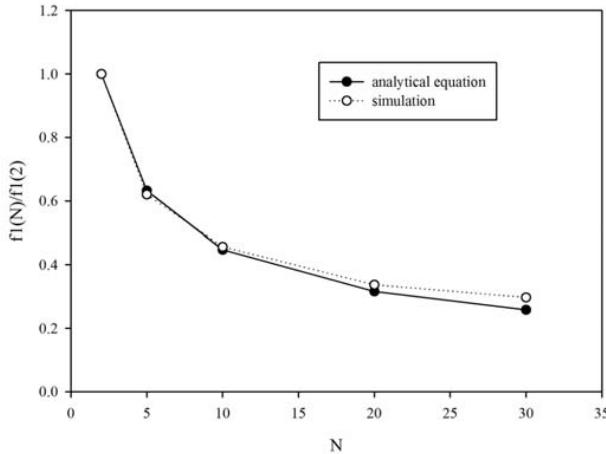

Figure 9. Comparison of frequency shift of the first oscillation mode dependences obtained by analytical equations (solid line) and electromagnetic simulation (dash line).
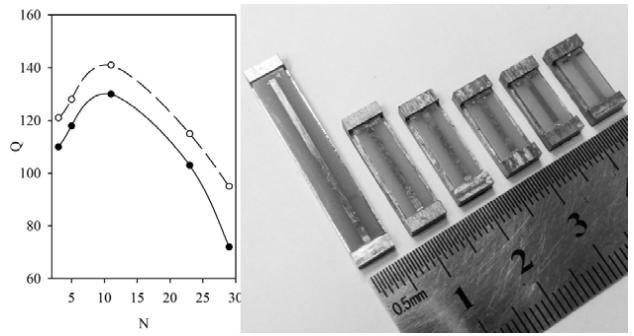

Figure 10. Q-factor behavior on changing N. Dashed line for the measured values and solid line for the simulation results. The fabricated resonators in comparison to regular $\lambda/4$ resonator (extreme left resonator).

Second, the proposed resonator is more compact than the ordinary microstrip one with the same width and eigenfrequency. For example, an ordinary $\lambda/4$ resonator of 2 mm width has 28.1 mm length. At the same time, the proposed resonator of the same width is more than 10 times shorter (2.6 mm). Thus, a 10 times smaller resonator has nearly the same Q-factor as a regular resonator.

In the resonator with a 1 μm gap between fingers, with the width changing from 0.2 to 4 mm, the optimal N is magnified from 19 to 512.

To prove the results obtained during the simulations, a set of resonators on 1 mm alumina substrate was fabricated. The set had five resonators containing 3, 5, 11, 23, and 29 fingers with 20 μm gaps between them. Their photo is presented in Fig. 10. The expected maximum Q-factor for this gap corresponds (accordingly with (15) to 11 fingers, and this is proven by the simulation and measurements

results carried out on the fabricated resonators (Fig. 10).

The measured Q-factors of the resonators appear higher (5–10%) that the simulated ones. In our opinion, this discrepancy originates from the fact that the used simulator does not take into account the distribution of MW current density correctly, particularly, the software does not take into account currents flowing in the sidewalls of the resonator.

4. EXPERIMENTAL RESULTS

Previously [26], for a designed and fabricated structure, inside the stopband between the first and second (spurious) passbands, there exist a number of spurious resonances that decrease the suppression level and width of the stopband. The resonances are excited in the fingers, and their number corresponds to the number of fingers in the resonator. Therefore, an investigation was carried out to get an opportunity of expanding a stopband and increasing its suppression level.

A galvanic interconnection of free ends of individual fingers in the structure suppresses the spurious resonances. The way of connection is presented in Fig. 11 for a 5-finger resonator. For example, connecting the first and last fingers in the resonator, we achieve a suppression of the first parasitic resonance. An interconnection of the first, last, and central fingers leads to the suppression of the first and second parasitic resonances. It should be noted that a connection should be made between the free ends of each of the two comb structures forming an interdigital resonator. It is obvious that such connection changes the eigenfrequency of the resonator; however, this influence does not disturb the passband of the filter significantly, so only a slight trimming after the connection is required. An interconnection of all fingers in the structure leads to the suppression of all spurious resonances inside the stopband. However, in this case, an average suppression level in the stopband becomes worse.

The above-mentioned scenario is illustrated in Figs. 13 and 14, where the frequency characteristics of a four-pole bandpass filter based on 21-pin resonator are shown. The filter was designed on a 1 mm alumina substrate for a central frequency of ~ 1000 MHz with the help of electromagnetic simulation. Each resonator has 1.04 mm width and 7.1 mm length and consists of 21 fingers of 40 μm width separated by 10 μm gaps. The chosen number of fingers is close to the optimal one according to the analytical equations. The spacing between the inner resonators was 2.09 mm, and the ones between the inner and outer resonators were 1.63 mm. The tapping of the filter to feed lines was chosen at the 0.6 mm from the open ends of the edge fingers in the outer resonators. The lateral sizes of the filter were found to be 11.1×7.1 mm, which corresponds to $0.0336\lambda_g \times 0.0204\lambda_g$ for the chosen central frequency. The topology of the filter is presented in Fig. 12. The designed filter has 10% of the fractional bandwidth and 1.7 dB of the minimal in-band insertion loss. Its frequency responses in the narrow- and wide-frequency bands are presented in Fig. 13.

One can see that the filter has the second (spurious) passband at a frequency higher than 7 GHz ($7f_0$); however, inside the stopband, one can see a significant number of spurious resonances, and
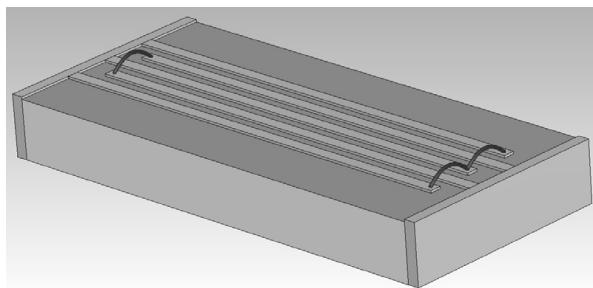

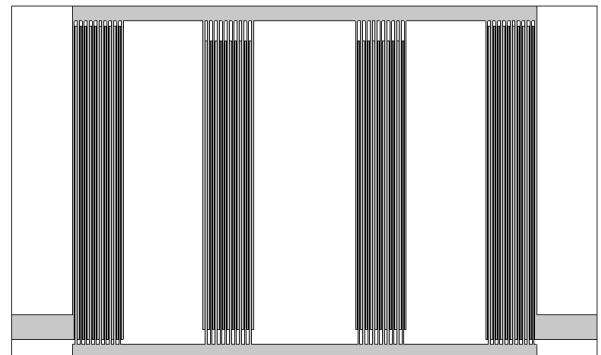**Figure 11.** A galvanic interconnection of free ends of individual fingers in 5 finger resonator.

Figure 12. Topology of 21 finger bandpass filter with a central frequency of 1 GHz.
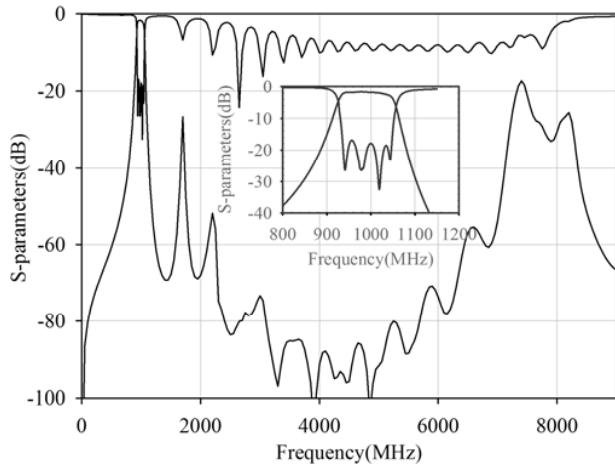
Figure 13. Frequency response of a designed filter in a wide-frequency range. A passband in a narrow-frequency range is shown in the inset.
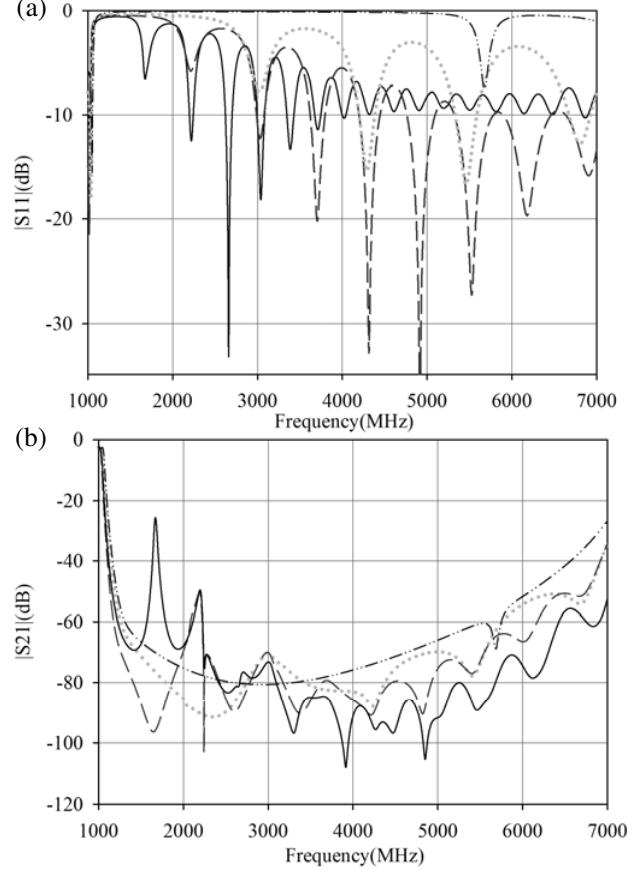
Figure 14. (a) Return loss and (b) insertion loss of the filter for cases: (1) no interconnection between the fingers (solid line), (2) the outer fingers in each of the resonators are interconnected (dashed line), (3) the outer and central fingers in each of the resonators are interconnected (dotted line), and (4) all fingers are interconnected in each resonator (dashed-dotted-dotted line).

at least 16 can be calculated from the S_{11} characteristic. The two closest to the passband spurious resonances have frequencies of 1.7 and 2.2 GHz and peak levels of -27 and -50 dB, respectively, making the performance poor. The simulation with the help of AWR Microwave Office has shown that the suppression of spurious resonances in the designed filter can be achieved by three ways: (1) two outer fingers in both comb structures in all resonators are interconnected, (2) the outer and central fingers in both comb structures in all resonators are interconnected, and (3) all fingers in both comb structures in all resonators are interconnected.

These statements are proven by simulation whose results are presented in Fig. 14(a) (S_{11}) and Fig. 14(b) (S_{21}). To simplify the perception, the results are presented only in the stopband of the filter. For a comparison, the figures also contain the results according to the filter without any interconnections. One can see that, in the first case, a significant suppression (> 70 dB) of the first spurious resonance (1.7 GHz) is observed. Also, due to the interconnection, a suppression of all odd spurious resonances occurs, as seen in the results of S_{11}. However, in this case, a general level of suppression in the high-frequency part of the stopband becomes less.

In the second case, along with 50 dB suppression of the first spurious resonance, a 40 dB suppression of the second spurious resonance (2.2 GHz) is seen, and additional sparseness of the spurious spectrum

is observed.

Finally, in the third case, only one spurious resonance exists in the high-frequency part of the stopband that does not narrow the stopband band. However, at the same time, a 20 dB decrease in its depth is observed.
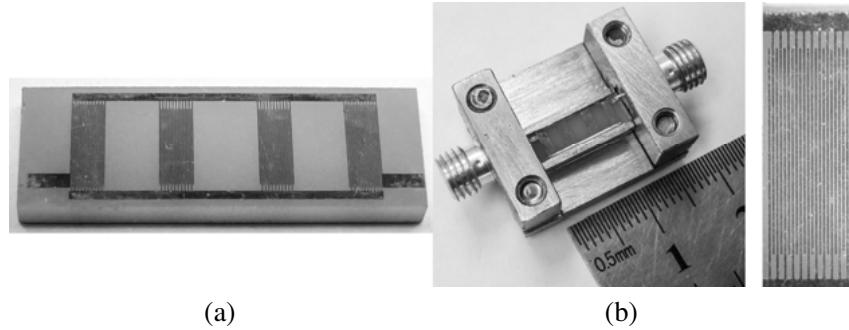

(a)   (b)

Figure 15. (a) Topology of the fabricated 4-pole bandpass filter with a central frequency of 2 GHz; (b) photograph of the fabricated filter and magnification of the resonator.

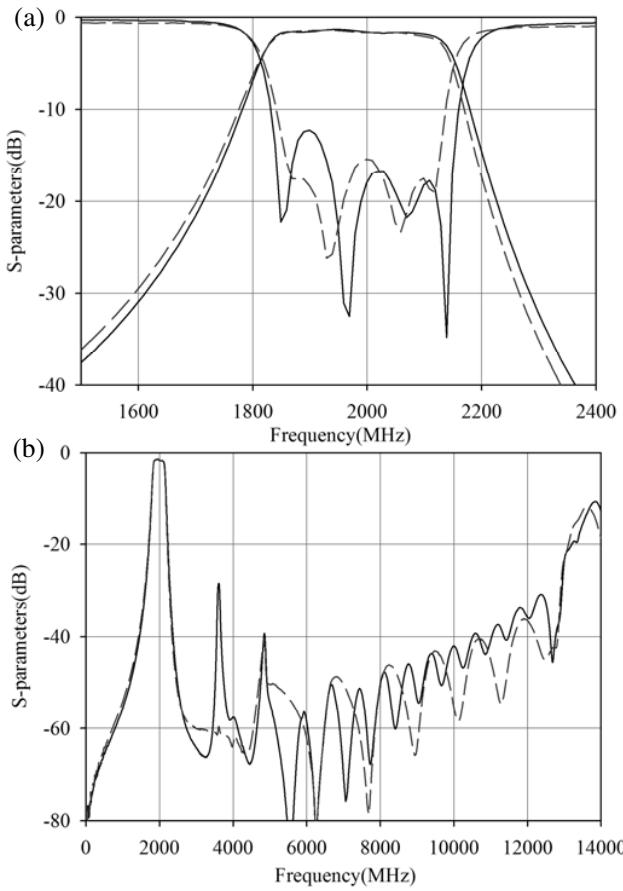**Figure 16.** Comparison of frequency responses of the fabricated filter containing interconnections of the fingers (dashed line) to the one without interconnections (solid line).
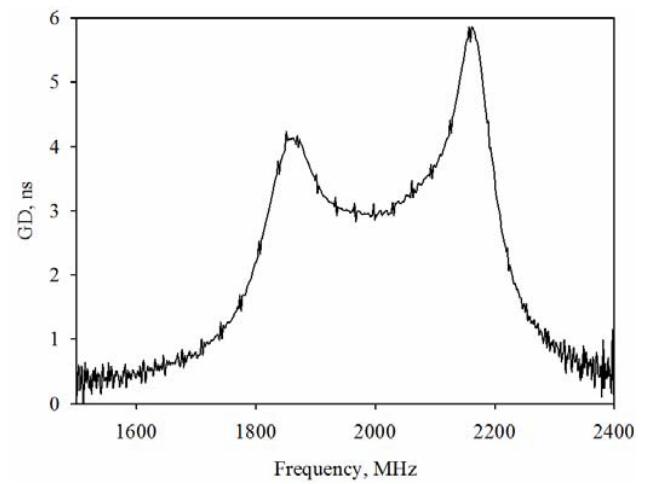
Figure 17. The measured group delay of the fabricated filter.

5. BANDPASS FILTER

In practice, the suppression of only the first and second spurious resonances is required because the others are of small intensity. A four-pole bandpass filter was designed and fabricated using a 1-mm-thick alumina substrate to prove the facts discovered during the investigation. The topology of the filter is presented in Fig. 15. The first type of the finger's interconnection (the outer fingers) was applied. The central frequency of the filter was 2 GHz, and its fractional bandwidth was 16% (320 MHz). The spacing between the internal resonators was 2.08 mm, whereas that between the external and internal ones was 1.59 mm. The chosen gaps between the fingers were 10 μm, which corresponds to the optimal number of fingers equal to 21. Therefore, for the 40 μm width of the fingers, the lateral sizes of the substrate were 11.5 mm × 3.8 mm or $0.077\lambda_g \times 0.025\lambda_g$. The filter tapping using two strips with a lateral size of 1.08 mm × 3.8 mm connected to the open ends of the outer fingers of the external resonators was done to match the filter with feed lines.

Photos of the fabricated filter and the magnification of its resonator are shown in Fig. 15. The removal of the interconnections has resulted in an frequency shift of external resonators, so the measured return loss of the filter was found to be less than 12 dB (Fig. 16, solid line). The first spurious resonance (unsuppressed) had a frequency of 3.67 GHz ($1.8f_0$) and a pick level of −29.3 dB.

Then, interconnections between the outer fingers in the external resonators were done using a 25 μm copper wire. The frequency responses for this case are demonstrated in Fig. 16 in narrow- and wide-frequency bands in comparison to the previous results.

The interconnections shift the external resonators frequency and correspondingly improve the level of in-band return loss, which is better than −15 dB. The measured minimal in-band insertion loss of the filter is found to be 1.3 dB.

According to the results measured in a wide-frequency range, the usage of interconnections suppresses the spurious resonances indeed. In Fig. 16(b), the first spurious resonance has lost 30 dB, widening the stopband according to the level −40 dB up to 11.0 GHz ($5.5f_0$). In addition, an expected sparseness of the spurious spectrum is observed.

The group delay behavior of the fabricated filter is presented in Fig. 17.

6. CONCLUSION

A microstrip resonator based on interdigital structure is proposed. It consists of two interdigital microstrip comb structures, and the common conductor of each "comb" is connected to the ground along its length. The unloaded Q-factor of the resonator has a square-root dependence on the number of fingers in the structure, and its eigenfrequency has a reversed square root dependence. The resonator possesses 2.5 times higher Q-factor than other miniaturized constructions described previously; such a behavior is explained based on the statement of high-frequency currents at the first resonant frequency flow in the same direction of all fingers of the interdigital structure. Therefore, the summary inductance of all fingers in the structure has nearly the same magnitude as the inductance of a single finger. In addition, the currents in the resonator are shared uniformly by all fingers, thus reducing the resistive loss in the resonator. However, an optimal number of fingers exists for each gap between them, which corresponds to the maximum value of the Q-factor. The maximum is a result of the confrontation of two trends: positive contribution of growing inductance with the negative one of growing resistance. In addition, in the case of the optimal number of fingers, the Q-factor of the resonator is practically the same as the Q-factor of a regular $\lambda/4$ resonator, whereas its length is more than an order of magnitude less.

It should be noted that the obtained equations can be used only to calculate the optimal number of fingers and the relative growth of Q-factor. At the same time, it is strongly limited in resonance position definition.

In bandpass filters based on the resonator, an extension of a high-frequency stopband can be achieved by interconnections of fingers in each of the two comb structures that bring suppression of spurious resonance spectra.

Fabricated resonators having different numbers of fingers and four-pole passband filter proved the simulation result. For the central frequency of 2000 MHz and 16.2% fractional bandwidth, the lateral

size of the filter is only $11.5\,\mathrm{mm} \times 3.8\,\mathrm{mm}$ ($0.077\lambda_g \times 0.025\lambda_g$) on alumina substrate ($\varepsilon = 9.8$). The filter has upper stopband up to $5.8f_0$ at the level $-40\,\mathrm{dB}$.

REFERENCES

1. Jin, X., W. Wen, and M. Chen, "Compact microstrip dual-/tri-/quad-band bandpass filter using open stubs loaded shorted stepped-impedance resonator," *IEEE Trans. Microw. Theory Tech.*, Vol. 61, No. 9, 3187–3199, Sep. 2013.

2. Shum, K. M., T. T. Mo, Q. Xue, and C. H. Chan, "A compact bandpass filter with two tuning transmission zeros using a CMRC resonator," *IEEE Trans. Microw. Theory Tech.*, Vol. 53, No. 3, 895–900, Mar. 2005.

3. Wu, C.-H., C.-H. Wang, and C. H. Chen, "Balanced coupled-resonator bandpass filters using multisection resonators for common-mode suppression and stopband extension," *IEEE Trans. Microw. Theory Tech.*, Vol. 55, No. 8, 1756–1763, Mar. 2007.

4. Mao, R.-J., X.-H. Tang, L. Wang, and G.-H. Du, "Compact hybrid resonator with series and shunt resonances used in miniaturized filters and balun filters," *IEEE Trans. Microw. Theory Tech.*, Vol. 56, No. 2, 440–448, Feb. 2008.

5. Liang, C.-H. and C.-Y. Chang, "Novel microstrip stepped-impedance resonator for compact wideband bandpass filters," *Asia Pacific Microwave Conference, APMC 2009*, 941–944, 2009.

6. Fernández-Prieto, A., A. Lujambio, J. Martel, F. Medina, F. Mesa, and R. R. Boix, "Simple and compact balanced bandpass filters based on magnetically coupled resonators," *IEEE Trans. Microw. Theory Tech.*, Vol. 63, No. 6, 1843–1853, Jun. 2015.

7. Luo, X., H. Qian, J.-G. Ma, K. Ma, and K. S. Yeo, "Compact dual-band bandpass filters using novel embedded spiral resonator (ESR)," *IEEE Microw. Compon. Lett.*, Vol. 20, No. 8, 435–437, Aug. 2010.

8. Chen, C.-F., T.-Y. Huang, and R.-B. Wu, "Novel compact net-type resonators and their applications to microstrip bandpass filters," *IEEE Trans. Microw. Theory Tech.*, Vol. 54, No. 2, 755–762, Feb. 2006.

9. Yang, T., M. Tamura, and T. Itoh, "Compact hybrid resonator with series and shunt resonances used in miniaturized filters and balun filters," *IEEE Trans. Microw. Theory Tech.*, Vol. 58, No. 2, 390–402, Feb. 2010.

10. Liang, C.-H. and C.-Y. Chang, "Compact wideband bandpass filters using stepped-impedance resonators and interdigital coupling structures," *IEEE Microw. Compon. Lett.*, Vol. 19, No. 9, 551–553, Sep. 2009.

11. Boonlom, K., T. Pratumvinit, and P. Akkaraekthalin, "A compact microstrip two-layers bandpass filter using improved interdigital-loop resonators," *IEEE International Symposium on Radio-Frequency Integration Technology, RFIT 2009*, 367–370, 2009.

12. Zhu, J. and Z. Feng, "Microstrip interdigital hairpin resonator with an optimal physical length," *IEEE Microw. Compon. Lett.*, Vol. 16, No. 12, 672–674, Dec. 2006.

13. Hong, J. S. and M. J. Lancaster, "Capacitively loaded microstrip loop resonator," *Electron. Lett.*, Vol. 30, No. 18, 1494–1495, Sep. 1994.

14. Aboush, Z. and A. Porch, "Compact, narrow bandwidth, lumped element bandstop resonators," *IEEE Microw. Compon. Lett.*, Vol. 15, No. 8, 524–526, Aug. 2005.

15. Liang, C.-H., C.-H. Chen, and C.-Y. Chang, "Fabrication-tolerant microstrip quarter-wave stepped-impedance resonator filter," *IEEE Trans. Microw. Theory Tech.*, Vol. 57, No. 5, 1163–1172, May 2009.

16. Jin, X., W. Wen, and M. Chen, "Compact and sharp skirts microstrip dual-mode dual-band bandpass filter using a single quadruple-mode resonator (QMR)," *IEEE Trans. Microw. Theory Tech.*, Vol. 61, No. 3, 1104–1112, Mar. 2013.

17. Bekheit, M., S. Amari, and W. Menzel, "Modeling and optimization of compact microwave bandpass filters," *IEEE Trans. Microw. Theory Tech.*, Vol. 56, No. 2, 420–430, Feb. 2008.

18. Athukorala, L. and D. Budimir, "Compact dual-mode open loop microstrip resonators and filters," *IEEE Microw. Compon. Lett.*, Vol. 19, No. 11, 698–700, Nov. 2009.

19. Tang, C.-W. and S.-F. You, "Design methodologies of LTCC bandpass filters, diplexer, and triplexer with transmission zeros," *IEEE Trans. Microw. Theory Tech.*, Vol. 54, No. 2, 717–723, Feb. 2006.

20. Ye, T., B. Yan, and S. Zhou, "A compact folded interdigital bandpass filter using LTCC technology," *2010 International Conference on Microwave and Millimeter Wave Technology, ICMMT*, 717–719, 2010.

21. Chen, H.-C., C.-H. Tsai, and T.-L. Wu, "A compact and embedded balanced bandpass filter with wideband common-mode suppression on wireless SIP," *IEEE Trans. Compon. Packag. Manuf. Technol.*, Vol. 2, No. 6, 1030–1038, Jun. 2012.

22. Tamura, M., T. Yang, and T. Itoh, "Very compact and low-profile LTCC unbalanced-to-balanced filters with hybrid resonators," *IEEE Trans. Microw. Theory Tech.*, Vol. 59, No. 8, 1925–1936, Aug. 2011.

23. Périgaud, A., S. Bila, S. Verdeyme, D. Baillargeat, and D. Kaminsky, "Multilayer interdigital structures for compact bandpass filters providing high selectivity and wideband rejections," *IEEE Microw. Compon. Lett.*, Vol. 24, No. 2, 93–95, Feb. 2014.

24. Belyaev, B. A., A. M. Serzhantov, V. V. Tyurnev, Y. F. Bal'va, and A. A. Leksikov, "Planar bandpass filter with 100-dB suppression up to tenfold passband frequency," *Progress In Electromagnetics Research C*, Vol. 48, 37–44, 2014.

25. Belyaev, B. A., A. M. Serzhantov, Ya. F. Bal'va, A. A. Leksikov, and R. G. Galeev, "A new design of a miniature microstrip resonator with interdigital structure," *Tech. Phys. Lett.*, Vol. 40, No. 11, 1010–1013, Nov. 2014.

26. Belyaev, B. A., A. M. Serzhantov, A. A. Leksikov, Ya. F. Bal'va, and A. A. Leksikov, "Novel high-quality compact microstrip resonator and its application to bandpass filter," *IEEE Microw. Compon. Lett.*, Vol. 25, No. 9, 579–581, Nov. 2015.

27. Leferink, F. B. J., "Inductance calculations; methods and equations," *IEEE International Symposium on Electromagnetic Compatibility*, 16–22, 1995.